

Uptake of ^{99m}Tc -tetrofosmin, ^{99m}Tc -MIBI and ^{201}Tl in malignant thymoma

Teisuke HASHIMOTO, Kazunori GOTO, Yuji HISHINUMA, Kazuhisa YACHUDA,
Yoshiaki SUGIOKA, Kazuhiro ARAI, Shusaku HARADA and Masabumi GOTO

Department of Radiology, Dokkyo University School of Medicine

^{99m}Tc -tetrofosmin, Thallium-201-chloride (^{201}Tl) and ^{99m}Tc -MIBI imagings were performed in a patient with malignant thymoma. Tracer uptake in the primary tumor was demonstrated. The tumor-to-background ratios of planar and SPECT imagings were 1.60 and 1.98 for ^{99m}Tc -tetrofosmin, 1.12 and 2.09 for ^{201}Tl , and 1.19 and 1.80 for ^{99m}Tc -MIBI, respectively. In another patient ^{99m}Tc -tetrofosmin and ^{201}Tl imagings were performed. Not only the primary tumor but also the direct invasions and metastatic lesions (bone metastases) were clearly detected. The tumor-to-background ratios of planar and SPECT imagings were 2.31 and 2.78 for ^{99m}Tc -tetrofosmin and 2.45 and 3.58 for ^{201}Tl , respectively. In ^{99m}Tc -tetrofosmin scintigraphy we acquired delayed images, and the tumor-to-background ratios of planar and SPECT delayed images were 1.20 and 1.86, the retention ratios were -1.11 and -0.92 and the retention indices were -48.1 and -33.1 , respectively. Our preliminary results suggest that ^{99m}Tc -tetrofosmin is useful in detecting not only the primary tumor but also metastatic lesions from malignant thymoma.

Key words: thymoma, ^{99m}Tc -tetrofosmin, ^{201}Tl , ^{99m}Tc -MIBI, SPECT

INTRODUCTION

^{99m}Tc -1,2-bis(bis(2-ethoxyethyl)phosphino)-ethane (tetrofosmin), a lipophilic monovalent cation, has recently been introduced as a new technetium-labeled pharmaceutical for myocardial perfusion studies. ^{99m}Tc -tetrofosmin and ^{99m}Tc -MIBI are now widely used in myocardial perfusion imaging. ^{201}Tl , a cationic material, is a useful tracer for detecting various tumors including thymoma. ^{99m}Tc -tetrofosmin as well as ^{99m}Tc -MIBI have shown potential utility as a tumor imaging agent for parathyroid adenoma,¹ breast cancer,^{2–4} lung cancer,^{5–8} thyroid cancer^{9,10} and other tumors.^{11,12} We report patients with malignant (invasive) thymoma who underwent ^{201}Tl , ^{99m}Tc -MIBI and ^{99m}Tc -tetrofosmin imagings.

CASE REPORTS

Case 1

A sixty-seven-year-old man entered our hospital complaining of double vision and right eyelid ptosis. A tensilon test was positive and a clinical diagnosis of myasthenia gravis was made. Thoracic CT revealed an anterior mediastinal tumor (Fig. 1). The result of CT guided biopsy was a malignant thymoma. We obtained informed consent from the patient. ^{99m}Tc -tetrofosmin and ^{201}Tl imagings were performed. The patient was injected with ^{99m}Tc -tetrofosmin (740 MBq) and underwent planar and SPECT imagings 10 min after the injection. ^{201}Tl (222 MBq) was injected and planar and SPECT imagings were performed 10 min after the injection. A large field of view dual detector gamma camera and computer system (GCA7200A, Toshiba) equipped with low-energy, high resolution, parallel hole collimators were used. Anterior and posterior simultaneous planar images (512 × 512 matrix, 1500 k counts) were acquired. The energy discriminator was centered on 71 keV for ^{201}Tl and 140 keV photopeak for ^{99m}Tc with a 20% window. Subsequently single photon emission computed tomography (SPECT)

Received December 8, 1999, revision accepted February 2, 2000.

For reprint contact: Teisuke Hashimoto, M.D., Department of Radiology, School of Medicine, Dokkyo University, 880 Kitakobayashi, Mibu-machi, Shimotsuga, Tochigi 321–0293, JAPAN.

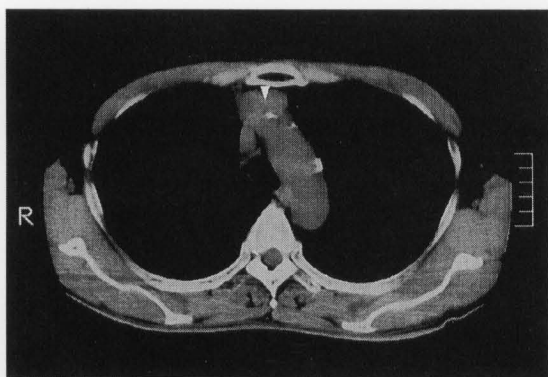


Fig. 1 A 67-year-old man with a malignant thymoma. Thoracic CT revealed a anterior mediastinal tumor (arrow head).

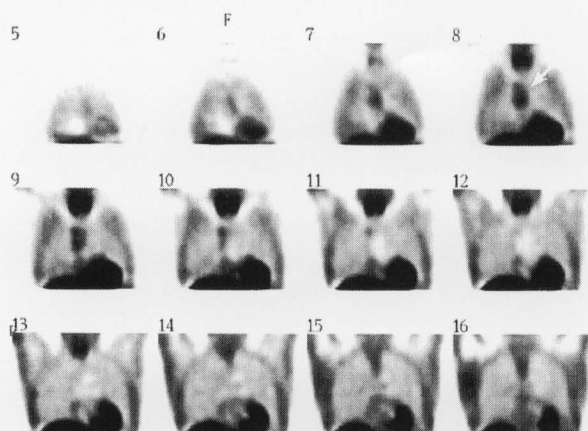


Fig. 2 Thoracic coronal SPECT images of ^{99m}Tc -tetrofosmin show intense tracer uptake in anterior mediastinal tumor (arrow).

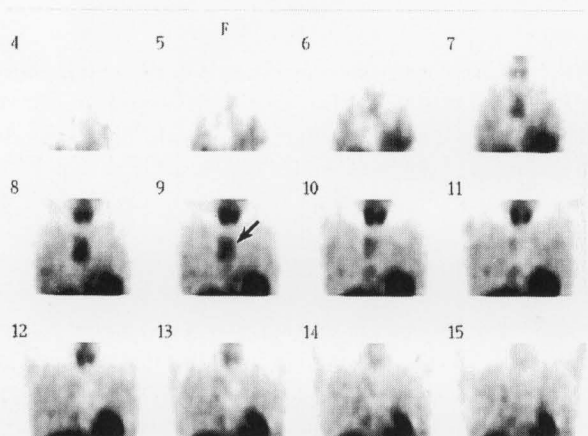


Fig. 3 Thoracic coronal SPECT images of ^{201}Tl show the accumulation of tracer in the tumor (arrow).

data were acquired. The dual detector gamma camera rotated through 180° in a circular orbit in 60 steps of 50 sec each for ^{201}Tl and ^{99m}Tc SPECT. Butterworth and Shepp & Logan filters were used to reconstruct tomographic

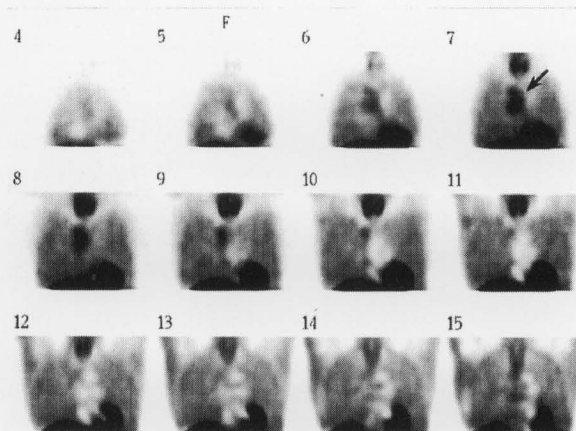


Fig. 4 Thoracic coronal SPECT images of ^{99m}Tc -MIBI show tumor uptake of tracer in the tumor (arrow).

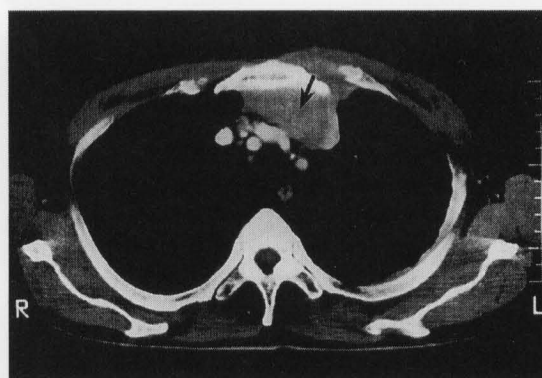


Fig. 5 A 66-year-old man with a malignant thymoma. Thoracic CT revealed a large anterior mediastinal tumor (arrow).

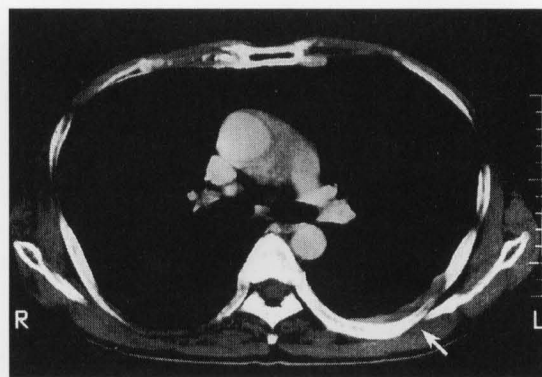


Fig. 6 Thoracic CT revealed an anterior mediastinal tumor and involvement of adjacent mediastinal structures (aorta), pleural disseminations and rib invasions.

images. The parameter of Butterworth filter was order 8, and the cut-off frequency was 0.15 cycles/pixel for both tracers. As seen in Figures 2, 3 and 4, thoracic coronal SPECT images of ^{99m}Tc -tetrofosmin, ^{201}Tl and ^{99m}Tc -

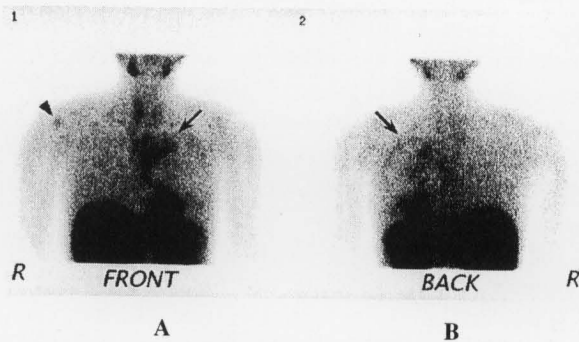


Fig. 7 ^{99m}Tc -tetrofosmin thoracic anterior planar image (Fig. 7A on the left) shows increased tracer uptake in primary mediastinal tumor (arrow) and right humeral bone metastasis (arrow heads). Posterior thoracic planar image (Fig. 7B on the right) shows the bone metastases of ribs and thoracic vertebrae and direct rib invasions from pleural disseminations of malignant thymoma (arrow).

MIBI show the accumulation of each tracer in the tumorous lesion corresponding to the anterior mediastinal tumor on X-ray CT. The tumor-to-background ratios of planar and SPECT imagings were 1.60 and 1.98 for ^{99m}Tc -tetrofosmin, 1.12 and 2.09 for ^{201}Tl , and 1.19 and 1.80 for ^{99m}Tc -MIBI, respectively.

Case 2

A sixty-six-year-old man came our hospital because abnormal pleural thickening was pointed out in a routine chest X-ray. Thoracic CT revealed an anterior mediastinal tumor (Fig. 5) and involvement of the sternum, subcutaneous fat tissue and adjacent mediastinal structures (aorta), pleural disseminations and rib invasions (Fig. 6). The result of CT guided biopsy indicated an invasive thymoma. We obtained informed consent from the patient. ^{99m}Tc -tetrofosmin, ^{201}Tl and ^{99m}Tc -MIBI imagings were performed. The patient was injected with ^{99m}Tc -tetrofosmin (740 MBq) and underwent planar and SPECT imagings 10 min and 3 hours after the injection. ^{201}Tl (222 MBq) and ^{99m}Tc -MIBI (740 MBq) were injected for the patient. Planar and SPECT imagings were obtained 10 min after the administration of both tracers. A ^{99m}Tc -tetrofosmin thoracic anterior planar image showed increased tracer uptake in the primary mediastinal tumor and right humeral bone metastasis (Fig. 7A). A posterior thoracic planar image showed ribs and thoracic vertebral bone metastases and direct rib invasions from pleural disseminations of malignant thymoma (Fig. 7B). Thoracic coronal SPECT (Fig. 8A) and transaxial SPECT (Fig. 8B) images of ^{99m}Tc -tetrofosmin clearly showed intense tracer activity in the primary anterior mediastinal tumor, direct sternum and subcutaneous fat tissue invasions and involvement of adjacent mediastinal structures (aorta, superior vena cava, mediastinum and pericardium), pleural disseminations and bone metastases in the rt humeral bone, ribs and thoracic vertebrae. Thoracic

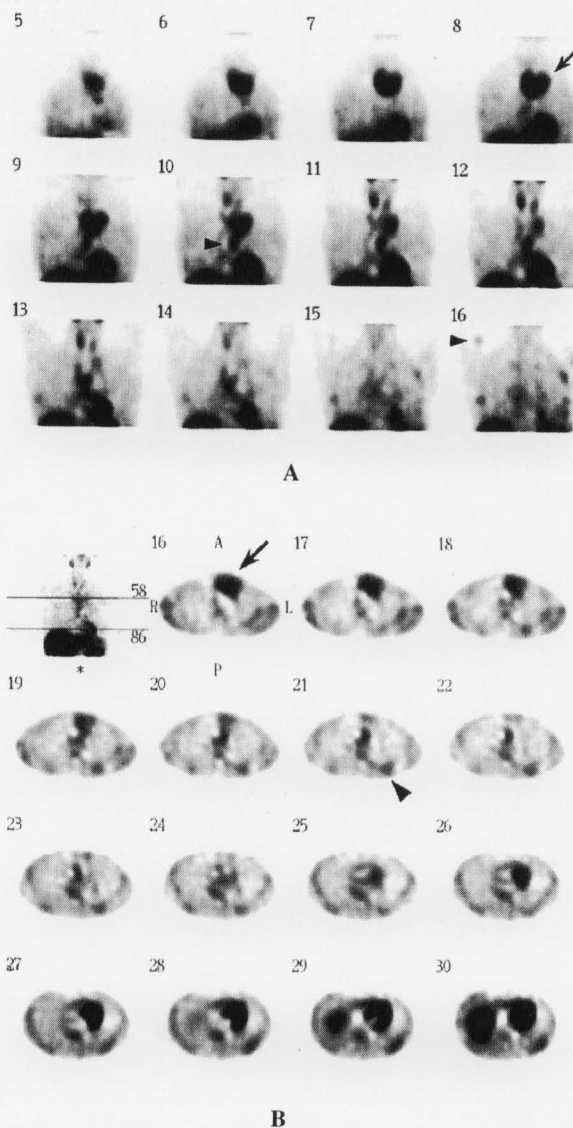


Fig. 8 Thoracic coronal SPECT (Fig. 8A) and transaxial SPECT (Fig. 8B) images of ^{99m}Tc -tetrofosmin clearly show intense tracer activity in primary anterior mediastinal tumor, direct sternum and subcutaneous fat tissue invasions and adjacent mediastinal invasions (aorta, superior vena cava and pericardium), pleural disseminations and bone metastases (rt humeral bone, ribs and thoracic vertebrae).

coronal SPECT (Fig. 9A) and transaxial SPECT (Fig. 9B) images of ^{201}Tl show tracer uptake in the primary tumor, direct sternum and subcutaneous fat tissue invasions and adjacent mediastinal invasions (aorta, superior vena cava and pericardium), pleural disseminations and bone metastases (rt humeral bone, ribs and thoracic vertebrae). The tumor-to-background ratios of planar and SPECT imagings were 2.31 and 2.78 for ^{99m}Tc -tetrofosmin, and 2.45 and 3.58 for ^{201}Tl , respectively. In ^{99m}Tc -tetrofosmin scintigraphy we acquired delayed images, and tumor-to-background ratios of planar and SPECT delayed images were 1.20 and 1.86, the retention ratios were -1.11

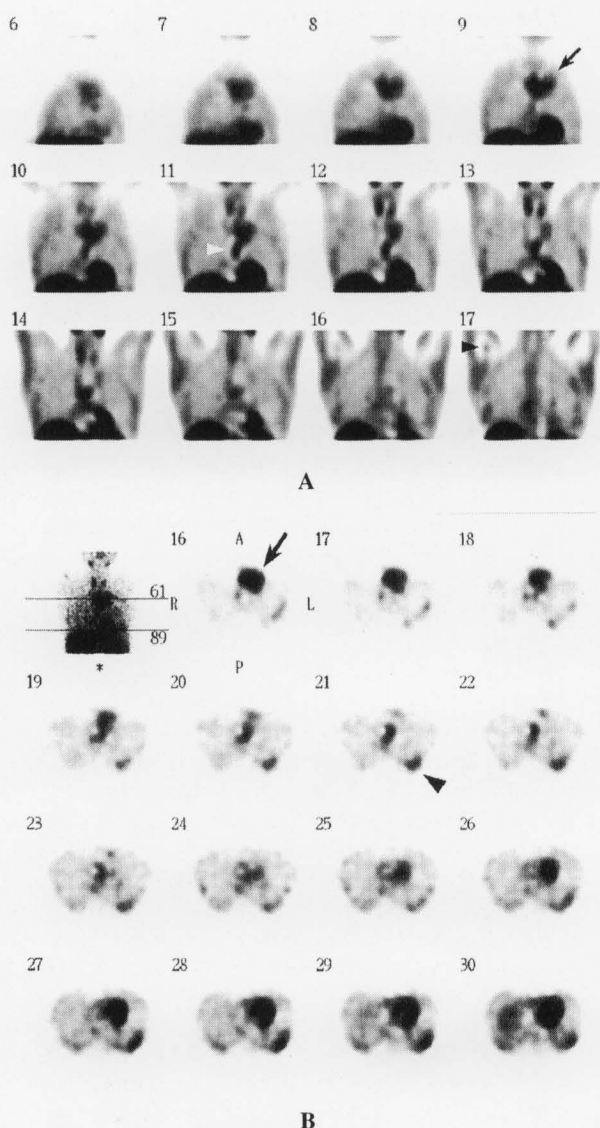


Fig. 9 Thoracic coronal SPECT (Fig. 9A) and transaxial SPECT (Fig. 9B) images of ^{201}Tl show tracer uptake in primary tumor, direct sternum and subcutaneous fat tissue invasions and adjacent mediastinal invasions (aorta, superior vena cava and pericardium), pleural disseminations and bone metastases (rt humeral bone, ribs and thoracic vertebrae).

and -0.92 , and retention indices were -48.1 and -33.1 , respectively. The retention ratio was obtained as follows: Delayed ratio $-$ Early ratio. The retention index was obtained by means of the following equation: Delayed ratio $-$ Early ratio/Early ratio $\times 100$.

DISCUSSION

^{201}Tl uptake of various tumors has been reported including malignant and benign thymic tumor.^{13,14} The tumor seeking properties of $^{99\text{m}}\text{Tc}$ -MIBI are also well known.¹⁵⁻¹⁷ $^{99\text{m}}\text{Tc}$ -tetrofosmin has recently been used as a new myocardial perfusion imaging agent, and has also

shown potential utility as a tumor imaging agent for such conditions as parathyroid adenoma,¹ breast cancer,²⁻⁴ lung cancer,⁵⁻⁸ thyroid cancer^{9,10} and other tumors.^{11,12} Although $^{99\text{m}}\text{Tc}$ -tetrofosmin uptake in mediastinal tumor was reported,¹⁸ there is no report on $^{99\text{m}}\text{Tc}$ -tetrofosmin uptake in bone and distant metastases from malignant thymoma.

There are several physical limitations to ^{201}Tl . The energy emitted is lower, the half-life is longer and the radiation dose to the patient is relatively higher. Compared with ^{201}Tl , $^{99\text{m}}\text{Tc}$ has some advantages over ^{201}Tl such as higher emitted energy, shorter half-life, smaller radiation dose, larger injected dose and better image quality.

As for the tumor-to-background (normal lung) ratio, in the planar images of case 1, the tumor-to-background ratio of the $^{99\text{m}}\text{Tc}$ -tetrofosmin (1.60) and $^{99\text{m}}\text{Tc}$ -MIBI (1.19) was superior to that of ^{201}Tl (1.12). But the tumor-to-background ratio of the SPECT images, $^{99\text{m}}\text{Tc}$ -tetrofosmin (1.98) and $^{99\text{m}}\text{Tc}$ -MIBI (1.80) was inferior to that of ^{201}Tl (2.09). In the planar images of case 2, the tumor-to-background ratio of the $^{99\text{m}}\text{Tc}$ -tetrofosmin (2.31) was inferior to that of ^{201}Tl (2.45) and in the SPECT images the tumor-to-background ratio of the $^{99\text{m}}\text{Tc}$ -tetrofosmin (2.78) was also inferior to that of ^{201}Tl (3.58). The ^{201}Tl tumor-to-background ratio was greater than that of $^{99\text{m}}\text{Tc}$ -tetrofosmin. This might be due to $^{99\text{m}}\text{Tc}$ -tetrofosmin showing higher uptake than ^{201}Tl in the normal lung. The $^{99\text{m}}\text{Tc}$ -tetrofosmin tumor-to-background ratio was greater than that of $^{99\text{m}}\text{Tc}$ -MIBI, and this might be due to $^{99\text{m}}\text{Tc}$ -tetrofosmin being cleared faster than $^{99\text{m}}\text{Tc}$ -MIBI¹⁹ from both the lungs and liver. Despite the better physical properties and imaging quality of $^{99\text{m}}\text{Tc}$, it is disappointing that $^{99\text{m}}\text{Tc}$ -tetrofosmin did not always outperform ^{201}Tl in the tumor-to-background ratio. But $^{99\text{m}}\text{Tc}$ -tetrofosmin was judged to be comparable to ^{201}Tl on visual estimation and almost comparable to ^{201}Tl as to its tumor-to-background ratio also.

The early tumor-to-background ratios calculated from $^{99\text{m}}\text{Tc}$ -tetrofosmin planar and SPECT images were higher than the delayed ratios, suggesting that the early imaging with $^{99\text{m}}\text{Tc}$ -tetrofosmin might be the better choice for detecting malignant thymoma.

^{201}Tl is a K^+ analogue. The uptake of ^{201}Tl by cells is related to cell membrane potential and Na^+ , K^+ ATPase activity and might involve other K^+ channels.^{20,21} ^{201}Tl remains in the cytosolic compartment,²¹ whereas $^{99\text{m}}\text{Tc}$ -MIBI is localized mostly inside mitochondria due to negative mitochondrial membrane potential,^{22,23} $^{99\text{m}}\text{Tc}$ -tetrofosmin is a monovalent lipophilic cation that rapidly enters the myocardial cells due to its lipophilic properties.^{24,25} The uptake of both $^{99\text{m}}\text{Tc}$ -tetrofosmin and $^{99\text{m}}\text{Tc}$ -MIBI is related to the Na^+ , K^+ pump, and Na^+/K^+ antiport systems.²⁶

The mechanism of uptake of $^{99\text{m}}\text{Tc}$ -MIBI and $^{99\text{m}}\text{Tc}$ -tetrofosmin into malignant cells and its exact localization

are not yet clear. The uptake of both tracers is known to depend on regional blood flow and on the mitochondrial content,²⁷ because ^{99m}Tc-MIBI and ^{99m}Tc-tetrofosmin *in vitro* studies,²⁸ appear to indicate that there is a connection with the multidrug resistance of P-glycoprotein, the 170-kDa protein coded by MDR1 (mammalian multidrug resistance gene). In addition, it was reported that accumulation of ^{99m}Tc-tetrofosmin in breast tumor cells *in vitro* is related to a p-glycoprotein similar to ^{99m}Tc-MIBI.²⁸

The chemosensitivity of a tumor is important for its management. Increased expression of transmembranous p-glycoprotein, the product of multidrug resistance 1 gene, has resulted in multidrug resistance. The multidrug resistance p-glycoprotein system functions as an energy dependent efflux pump which reduces the amount of intracellular transporting cytotoxic agents, MIBI and tetrofosmin, in tumor cells. The accumulations of ^{99m}Tc-MIBI and ^{99m}Tc-tetrofosmin are inversely proportional to the level of p-glycoprotein expression.²⁹⁻³¹ Therefore the accumulation of ^{99m}Tc-tetrofosmin in tumors provides us not only with the localization of the primary tumor and metastatic lesions but also the chemosensitivity of the tumor, which may predict the response to chemotherapy and selection of therapy management.

In conclusion, ^{99m}Tc-tetrofosmin imaging would be helpful in detecting both the primary tumor and metastatic lesions from malignant thymoma. Further investigations and larger clinical trials are needed to justify the potential usefulness of this tracer as a tumor detecting imaging agent.

REFERENCES

1. Ishibashi M, Nishida H, Hiromatsu Y, Kojima K, Tabuchi E, Hayabuchi N. Comparison of technetium-99m MIBI, technetium-99m-tetrofosmin, ultrasound and MRI for localization of abnormal parathyroid glands. *J Nucl Med* 39: 320-324, 1998.
2. Rambaldi PE, Mansi L, Procaccini E, Di Gregorio F, Del Vecchio E. Breast cancer detection with ^{99m}Tc-tetrofosmin. *Clin Nucl Med* 20: 703-705, 1995.
3. Mansi L, Rambaldi PF, Procaccini E, Di Gregorio F, Laprovietera A, Pecori B, et al. Scintimammography with technetium-99m tetrofosmin in the diagnosis of breast cancer and lymph node metastases. *Eur J Nucl Med* 23: 932-939, 1996.
4. Takayama T, Kinuya S, Sugiyama M, Hashiba A, Takeda R, Tonami N. ^{99m}Tc-tetrofosmin uptake in bone metastases from breast cancer. *Ann Nucl Med* 12: 293-296, 1998.
5. Basoglu T, Sahin M, Coskun C, Koparan A, Bernay I, Erkan L. Technetium-99m-tetrofosmin uptake in malignant lung tumours. *Eur J Nucl Med* 22: 687-689, 1995.
6. Matsunari I, Kinuya S, Nishikawa T, Matoba M, Murakita K, Ohguchi M, et al. Technetium-99m tetrofosmin uptake in lung cancer: comparison with thallium-201. *Ann Nucl Med* 10: 143-145, 1996.
7. Schillaci O, Danieli R, Tavolaro R, Scopinaro F. ^{99m}Tc-tetrofosmin accumulation in lung cancer and its metastases. *Clin Nucl Med* 22: 46-47, 1997.
8. Takekawa H, Takaoka K, Tsukamoto E, Kanegae K, Kozeki Y, Yamaya A, et al. Visualization of lung cancer with ^{99m}Tc-tetrofosmin imaging: comparison with ²⁰¹Tl. *Nucl Med Commun* 18: 341-345, 1997.
9. Kosuda S, Yokoyama H, Katayama M, Yokokawa T, Kusano S, Yamamoto O. Technetium-99m tetrofosmin and technetium-99m sestamibi imaging of multiple metastases from differentiated thyroid carcinoma. *Eur J Nucl Med* 22: 1218-1220, 1995.
10. Lind P, Gallowitsch HJ, Langsteger W, Kresnik E, Mikosch P, Gomez I. Technetium-99m-tetrofosmin whole-body scintigraphy in the follow-up of differentiated thyroid carcinoma. *J Nucl Med* 38: 348-352, 1997.
11. Kostakoglu L, Uysal U, Ozyar E, Demirkazik FB, Hayran M, Atahan L, et al. A comparative study technetium-99m sestamibi and technetium-99m tetrofosmin single-photon tomography in the detection of nasopharyngeal carcinoma. *Eur J Nucl Med* 24: 621-628, 1997.
12. Soderlund V, Jonsson C, Bauer HCF, Brosjo O, Jacobsson H. Comparison of technetium-99m-MIBI and technetium-99m-tetrofosmin uptake by musculoskeletal sarcomas. *J Nucl Med* 38: 682-686, 1997.
13. Tonami N, Shuke N, Yokoyama K, Seki H, Takayama T, Kinuya S, et al. Thallium-201 single photon emission computed tomography in the evaluation of suspected lung cancer. *J Nucl Med* 30: 997-1004, 1989.
14. Fukuda T, Itami M, Sawa H. A case of thymoma arising from undescending thymus-high uptake of thallium-201 chloride. *Eur J Nucl Med* 5: 465-468, 1980.
15. Aktolun C, Bayhan H, Kir M. Clinical experience with Tc-99m MIBI imaging in patients with malignant tumors, preliminary results and comparison with Tl-201. *Clin Nucl Med* 17: 171-176, 1992.
16. Waxman A, Nagaraj N, Ashok G. Sensitivity and specificity of Tc-99m methoxy isobutyl isonitrile (MIBI) in the evaluation of primary carcinoma of the breast: Comparison of palpable and nonpalpable lesions with mammography. *J Nucl Med* 35: 22, 1994.
17. Ziegels P, Nocaude M, Hugo D, Deveaux M, Detournignies L, Wattel E, et al. Comparison of technetium-99m-methoxyisobutylisonitrile and gallium-67 citrate scanning in the assessment of lymphomas. *Eur J Nucl Med* 22: 126-131, 1995.
18. Isibashi M, Fujimoto K, Ohzono H, Meno S, Hayabuchi N. ^{99m}Tc tetrofosmin uptake in mediastinal tumours. *Brit J Radiol* 69: 1134-1138, 1996.
19. Higley B, Smith FW, Smith T, Gemmell HG, Gupta PD, Gvozdanovic DV, et al. Technetium-99m-1,2-bis[bis(2-ethoxyethyl)phosphino]ethane: Human biodistribution, dosimetry and safety of a new myocardial perfusion imaging agent. *J Nucl Med* 34: 30-38, 1993.
20. McCall D, Zimmer LJ, Katz AM. Kinetics of thallium exchange in culture rat myocardial cells. *Cir Res* 56: 370-376, 1985.
21. Brismar T, Collins VP, Kesselberg M. Thallium-201 uptake relates to membranous potential and potassium permeability in human glioma cells. *Brain Res* 500: 30-36, 1989.
22. Piwnica-Worms D, Kronauge JF, Delmon L. Uptake and retention of hexakis(2-methoxyisobutyl isonitrile) technetium (I) in cultured chick myocardial cells. *Circulation* 82:

- 1926–1938, 1990.
23. Carvalho PA, Chiu ML, Kronauge JF. Subcellular distribution and analysis of technetium-99m-MIBI in isolated perfused rat hearts. *J Nucl Med* 33: 1516–1521, 1992.
 24. Kelly JD, Forster AM, Higley B. Technetium-99m-tetrofosmin as a new radiopharmaceutical for myocardial perfusion imaging. *J Nucl Med* 34: 222–227, 1993.
 25. Mousa SA, Williams SJ, Sands H. Characterization of *in vivo* chemistry of cations in the heart. *J Nucl Med* 28: 1951–1957, 1987.
 26. Arbab AS, Koizumi K, Toyama K, Arai T, Araki T. Ion transport systems in the uptake of ^{99m}Tc -tetrofosmin, ^{99m}Tc -MIBI and ^{201}Tl in a tumour cell line. *Nucl Med Commun* 18: 235–240, 1997.
 27. Platts EA, North TL, Pickett RD. Mechanism of uptake of technetium-99m tetrofosmin. I: uptake into isolated adult rat ventricular myocytes and subcellular localization. *J Nucl Med* 37: 1578–1582, 1996.
 28. Ballinger JR, Banneman J, Boxen I. Technetium-99m-tetrofosmin as a substrate for p-glycoprotein: *in vitro* studies in multidrug-resistant breast tumor cells. *J Nucl Med* 37: 1578–1582, 1996.
 29. Cordobes MD, Starzec A, Delmon-Moingeon L. Technetium-99m-sestamibi uptake by human benign and malignant breast tumor cells: correlation with *mdr* gene expression. *J Nucl Med* 37: 286–289, 1996.
 30. Del Vecchio S, Ciarmiello A, Potena MI. *In vivo* detection of multidrug-resistant (MDR1) phenotype by technetium-99m sestamibi scan in untreated breast cancer patients. *Eur J Nucl Med* 24: 150–159, 1997.
 31. Fujii H, Nakamura K, Kubo A, Enomoto K, Ikeda T, Kubota T, et al. Preoperative evaluation of the chemosensitivity of breast cancer by means of double phase ^{99m}Tc -MIBI scintimammography. *Ann Nucl Med* 12: 307–312, 1998.